

Research Article

Cubic-to-Tetragonal Phase Transitions in Ag–Cu Nanorods

Francesco Delogu and Michele Mascia

Dipartimento di Ingegneria Chimica e Materiali, Università degli Studi di Cagliari, Piazza d'Armi, 09123 Cagliari, Italy

Correspondence should be addressed to Francesco Delogu, delogu@dicm.unica.it

Received 19 December 2011; Accepted 13 February 2012

Academic Editor: Grégory Guisbiers

Copyright © 2012 F. Delogu and M. Mascia. This is an open access article distributed under the Creative Commons Attribution License, which permits unrestricted use, distribution, and reproduction in any medium, provided the original work is properly cited.

Molecular dynamics simulations have been used to investigate the structural behavior of nanorods with square cross section. The nanorods consist of pure Ag and Cu phases or of three Ag and Cu domains in the sequence Ag–Cu–Ag or Cu–Ag–Cu. Ag and Cu domains are separated by coherent interfaces. Depending on the side length and the size of individual domains, Ag and Cu can undergo a transition from the usual face-centered cubic structure to a body-centered tetragonal one. Such transition can involve the whole nanorod, or only the Ag domains. In the latter case, the transition is accompanied by a loss of coherency at the Ag–Cu interfaces, with a consequent release of elastic energy. The observed behaviors are connected with the stresses developed at the nanorod surfaces.

1. Introduction

It is well known that surface and bulk atoms exhibit different properties due to their different coordination numbers [1, 2]. For example, surface atoms have a potential energy higher than bulk ones as a consequence of their smaller number of neighbors [1, 2]. It follows that the overall physical and chemical behavior of a given system depends on the fractions of surface and bulk atoms [1, 2], which are in turn affected by the characteristic system lengths [1–5]. Whenever at least one of these lengths is in the nanometer range, the fractions of surface and bulk atoms become comparable [1–5]. For this reason, nanometer-sized systems must be expected to exhibit unusual properties ascribable to surface effects [3–5].

One of the most striking examples of surface effects in nanometer-sized systems is provided by the change in the relative thermodynamic stability of different crystalline structures [6, 7]. Provided that the free energy difference between the crystalline structures is on the order of surface free energies, the crystalline phase thermodynamically less favored in the bulk can become the most stable one at the nanoscale [6, 7]. This is the case of Pd nanocubes compressed in a diamond anvil cell, which exhibit a face-centered tetragonal structure even though massive Pd under similar conditions keep the face-centered cubic (fcc) lattice [6]. Numerical simulations also indicate that isolated Ag and Au

nanorods (NRs) can exhibit a body-centered tetragonal (bct) structure, unstable in the bulk, due to intrinsic surface stresses [7, 8]. Along the same line, fcc Pd NRs have been shown to transform into either a bct or a hexagonal close-packed (hcp) structure [9, 10]. Other examples can be found in the behavior of Ni nanometer-sized systems [11, 12]. Experimental work has shown that highly strained hcp Ni islands form by heteroepitaxial growth on the (001) face of MgO [11], whereas numerical simulations have given the necessary theoretical support and extended the predictions to Co, Pd, and Pt [12]. Furthermore, it has been demonstrated that intrinsic surface stresses are sensitive to both surface composition and curvature [13–15].

Starting from the afore mentioned results, the present work aims at deepening the insight into the effect of chemical composition on the intrinsic surface stresses arising in NRs. Attention is focused on Ag and Cu NRs as well as on composite NRs with three alternate Ag and Cu domains according to the sequences Ag–Cu–Ag and Cu–Ag–Cu. Molecular dynamics simulations have been used to investigate the stability of the different NRs as a function of their cross-sectional area and, in the case of composite NRs, of the size of chemical domains. It is shown that the smallest Ag NRs exhibit an unusual bct structure. It is also shown that the presence of Cu domains can significantly affect the phase stability of Ag in composite NRs. Depending on the

composite NR size, Cu can also undergo a fcc-to-bct transition unobserved in both Cu bulk phases and NRs.

2. Computational Outline

Interactions were described by using a semiempirical tight-binding (TB) potential based on the second-moment approximation to the density of electronic states [16, 17]. Accordingly, the cohesive energy E is expressed as

$$E = \sum_{\alpha} \sum_{i_{\alpha}=1}^{N_{\alpha}} \left\{ \sum_{\beta} \sum_{j_{\beta}=1}^{N_{\beta}} A_{\alpha\beta} e^{-p_{\alpha\beta}((r_{ij}^{\alpha\beta}/d_{\alpha\beta})-1)} - \left[\sum_{\beta} \sum_{j_{\beta}=1}^{N_{\beta}} \xi_{\alpha\beta}^2 e^{-p_{\alpha\beta}((r_{ij}^{\alpha\beta}/d_{\alpha\beta})-1)} \right]^{1/2} \right\}, \quad (1)$$

where i_{α} and j_{β} run over the N_{α} and N_{β} atoms of species α and β , $r_{ij}^{\alpha\beta} = |r_{i\alpha} - r_{j\beta}|$ is the distance between two atoms, the parameters $A_{\alpha\beta}$, $\xi_{\alpha\beta}$, $p_{\alpha\beta}$, and $q_{\alpha\beta}$ quantify the potential energy, and $d_{\alpha\beta}$ is the distance between α - β nearest neighbor pairs at 0 K. The first member on the right-hand side describes the repulsive part of the potential as a Born-Mayer pairwise interaction, while the second member accounts for the attractive part in the framework of the second-moment approximation of the TB band energy [16, 17]. Interactions were computed within a cutoff distance r_c of 0.67 nm. The potential parameter values were taken from literature [17, 18].

The selected TB potential exhibits a remarkable capability in reproducing the structural, thermodynamic, and mechanical properties of both massive and nanometer-sized transition metals and their alloys [1, 2, 16–19]. It has been successfully employed to study Ag and Cu systems, including metastable solid solutions at the nanometer scale [1, 2, 16–19]. However, the present work has qualitative purposes, and the obtained results should be regarded as a rough approximation of real behavior.

Ag and Cu NRs as well as composite Ag–Cu–Ag and Cu–Ag–Cu ones were created starting from relaxed Ag and Cu bulk phases containing 256000 Ag or Cu atoms arranged in $40 \times 40 \times 40$ cF4 fcc elementary cells. The bulk systems were relaxed at 200 K in the isobaric-isothermal statistical ensemble with number of atoms, pressure, and temperature T constant [20, 21]. The Parrinello-Rahman scheme was employed to suitably deal with possible phase transitions [22]. Periodic boundary conditions were applied along the three Cartesian directions [23]. Equations of motion were solved with a fifth-order predictor-corrector algorithm [23] and a time step of 2 fs. The fluctuations of volume as well as of potential and kinetic energies were used to monitor the equilibration process, which attained completion after approximately 0.2 ns.

Five Ag NRs and five Cu NRs about 15 nm long and with square cross section were created by selecting parallelepipedic regions at the center of the Ag and Cu bulk phases, respectively. The side length s of the square cross section was given values roughly equal to 1.2, 1.6, 2.0, 2.4, and

2.8 nm. The NR main axis was chosen coincident with the $\langle 100 \rangle$ crystallographic direction, so that free surfaces exhibit (100), (010), and (001) crystallographic facets, respectively. The choice of investigating $\langle 100 \rangle$ NRs with (100), (010), and (001) crystallographic facets is motivated by the fact that only such orientation and facets allow the fcc-to-bct phase transition in Ag and Au NRs [7, 15, 24]. Although (111) crystallographic facets are in principle more stable than (100) ones [25], these seem to be necessary to reach intrinsic surface stresses large enough to affect the stability of the fcc crystalline phase and promote a change to the bct crystalline lattice.

The unsupported Ag and Cu NRs were obtained by isolating the selected parallelepipeds from the parent matrices. To such aim, the interactions between the atoms inside and outside the parallelepiped were progressively canceled by reducing linearly to zero in 50 ps, the A and ξ potential parameters for the involved atomic pairs.

Although computationally cumbersome, the afore mentioned procedure allows the gradual relaxation of NRs already during the process of formation [8, 18]. In particular, it permits equilibrating the excess energy appearing at free surfaces as a consequence of the disappearance of the matrix [8, 18]. Correspondingly, the unsupported NRs exhibit relaxed free surfaces [8, 18].

The unsupported Ag and Cu NRs were used to fabricate, respectively, the composite Ag–Cu–Ag and Cu–Ag–Cu NRs. The composite Ag–Cu–Ag NRs were created by selecting k atomic planes at the center of the Ag NRs and replacing the Ag atoms there located with Cu ones. An analogous procedure was followed to create the composite Cu–Ag–Cu NRs. The number k of Ag or Cu atomic planes defines the size of the central domains. It was given integer values in the range between 2 and 24, with consecutive values differing by two units. 72 being the total number of atomic planes included in any given NR, the number of atomic planes in the Ag or Cu end portions varied between 24 and 35. Information on the composite Ag–Cu–Ag NRs is given in Table 1.

The replacement of Ag atoms with Cu ones, and *vice versa*, induces a considerable strain at the Ag–Cu interfaces due to the different elementary cell parameters of Ag and Cu. The result is the formation of highly strained interfacial regions in which Ag and Cu lattices, even though affected by compressive and tensile respectively, keep the initial coherency [26].

Structural features were studied by comparing the distances and the spatial arrangement of neighboring atoms to point out any departure from the equilibrium fcc arrangement and to identify the attained crystalline structure [27].

The average stress f at the NR surfaces was estimated by the first derivatives of the interatomic potential [13]. Although relatively simple and direct, this method is sensitive to the shape of the potential curve [8, 13]. Therefore, small differences in the f values obtained by using different potentials must be expected. Also, it must be noted that the evaluation of the average surface stress f is further complicated by the presence of different chemical domains along

TABLE 1: The side length s , the cross-sectional area A_{NR} , the total number N of atoms and the total number N_{plane} of atoms in individual atomic planes. A_{NR} values refer to the initial configuration of the different composite Ag–Cu–Ag NRs investigated with fcc crystallographic structure. The NRs are about 15 nm long, that is, include 72 atomic planes perpendicular to the NR main axis. For each given NR, the number k of Cu atomic planes was varied of two units in the range between 2 and 24. The number N_{Cu} of Cu atoms in composite Ag–Cu–Ag NRs can be evaluated by the product of the number k of Cu atomic planes in the NR with the number N_{plane} of atoms in individual atomic planes. The number N_{Ag} of Ag atoms can be evaluated as the difference between the total number N of atoms in the NR and N_{Cu} .

s (nm)	A_{NR} (nm ²)	N	N_{plane}
1.2	1.44	1800	25
1.6	2.56	2952	41
2.0	4.00	4392	61
2.4	5.76	6120	85
2.8	7.84	8136	113

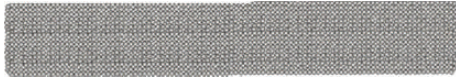


FIGURE 1: The relaxed atomic configuration of the unsupported Ag NR with sides about 2.8 nm long.

the NR axis, which results in an inhomogeneous distribution of local strains at the NR surfaces.

The induced compressive stress σ_{NR} along the NR axis can be indirectly estimated from the average surface stress f by calculating the ratio $4fl/A_{NR}$ [24], where l and A_{NR} represent, respectively, the total length and the cross-sectional area of NRs.

All of the results discussed in the following were obtained from at least two simulations, aimed at ascertaining the reliability of results and their dependence on the initial configuration.

3. Ag and Cu NRs

The relaxed atomic configuration of the unsupported Ag NR with sides about 2.8 nm long is shown in Figure 1. It can be seen that the system has kept the fcc crystalline structure typical of Ag bulk phases. The stability of this structure depends on the size of the NR. As observed in previous work [8], the fcc structure is replaced by a bct one as the side length s of the Ag NR becomes equal to 2.0 nm or smaller. The analysis of the atomic arrangements indicates that the bct structure exhibits elementary cell parameters a_{bct} and c_{bct} equal to about 0.347 and 0.286 nm, respectively.

Information on the mechanism of the phase transition is obtained by visualizing the atomic configurations of Ag NRs at different times. The images of a few configurations are shown in Figure 2. They clearly point out that the fcc-to-bct phase transition nucleates at the free (100) surfaces

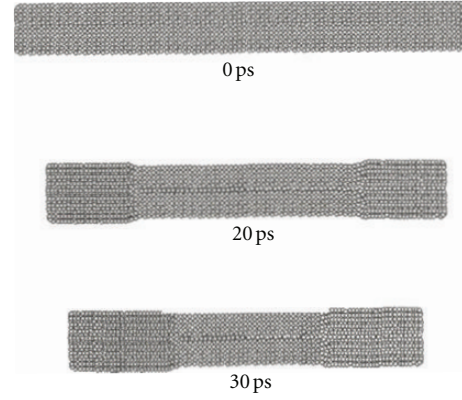


FIGURE 2: Atomic configurations of the Ag NR with side length s equal to about 2.0 nm taken at the indicated times.

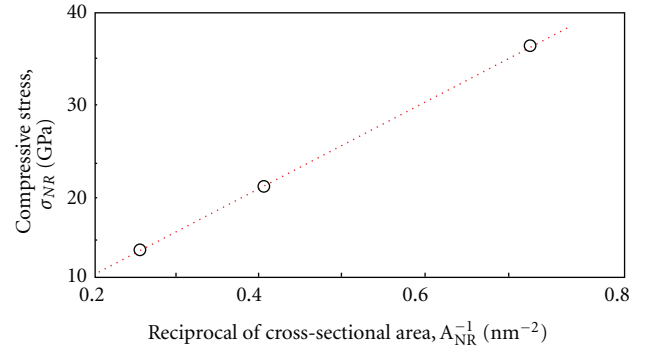


FIGURE 3: The surface-induced compressive stress σ_{NR} as a function of the reciprocal of the NR cross-sectional area A_{NR} , A_{NR}^{-1} . The best-fitted line is also shown.

perpendicular to the NR main axis and progressively propagates inwards at a rate of about 400 nm ns⁻¹.

Following previous work [7, 15], the fcc-to-bct phase transition in NRs with cross-sectional area A_{NR} smaller than about 4 nm² has been connected with the surface stress f . Calculations point out that the average surface stress f exhibited by the (100) free surfaces of the Ag NRs amounts approximately to -1.3 J m⁻². This f value is on the same order of magnitude than the ones reported in literature for Au nanowires [7]. The negative sign of the f estimate indicates that the Ag NRs undergo a contraction along their main axis. The extent to which their length contracts depends on the intensity of the compressive stress σ_{NR} induced by the surface stress f . The compressive stress σ_{NR} varies with the NR size as shown in Figure 3, where σ_{NR} is plotted as a function of the reciprocal of the NR cross-sectional area A_{NR} , A_{NR}^{-1} . The largest NR able to undergo the fcc-to-bct phase transition is the one with cross-sectional area A_{NR} equal to about 4 nm². In this case, the surface-induced compressive stress σ_{NR} amounts to about 13 GPa. This value can be also regarded as the minimum surface-induced compressive stress σ_{NR} able to promote a fcc-to-bct phase transition in Ag NRs with square cross section.

In contrast with the behavior exhibited by Ag NRs, Cu NRs do not undergo any fcc-to-bct phase transition. In all

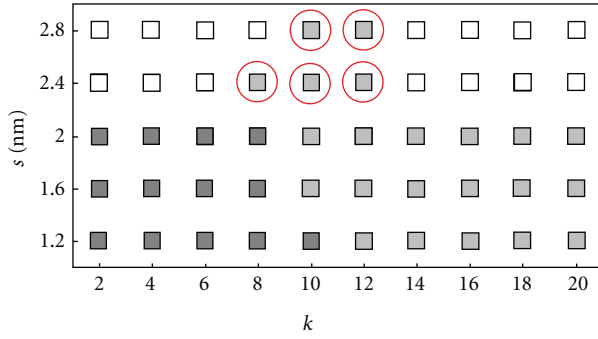


FIGURE 4: A grid showing the different combination of side length s and number k of Cu atomic planes for all of the composite Ag-Cu-Ag NRs considered. Dark and light gray indicate, respectively, the NRs entirely and partially involved in fcc-to-bct phase transitions. The red circles point out the NRs in which the fcc-to-bct phase transition of Ag end portions does not find counterpart in pure Ag NRs of the same size.

of the examined cases, that is, Cu NRs with roughly the same size of Ag NRs, the fcc structure exhibits the highest stability. Therefore, it is kept by all of the unsupported Cu NRs irrespective of their cross sectional area.

The behavior of Ag and Cu NRs described previously represents the starting point to analyze the behavior of composite Ag-Cu-Ag and Cu-Ag-Cu NRs.

4. Composite Ag-Cu-Ag NRs

In the case of Ag-Cu-Ag NRs, considerable lattice distortions are observed at the interfacial regions. On the one hand, the Cu side of the Ag-Cu interface undergoes a tensile deformation, which results in a cell parameter slightly larger than the equilibrium one. On the other hand, the Ag atoms at the interface are submitted to a compressive stress, and their local cell parameter is smaller than the equilibrium one. The same is true for all of the Ag-Cu-Ag NRs investigated.

The central Cu domain is expected to affect the fcc-to-bct phase transition behavior of the composite NRs. The stacking of k Cu atomic planes between the Ag domains can be regarded as a perturbation of the NR including only Ag atoms. The consequence of such perturbation can be readily visualized from the grid shown in Figure 4. The grid is constructed by correlating the NR side length s with the number k of Cu atomic planes and allows to mark the composite Ag-Cu-Ag NRs affected by structural changes. Four different regions can be identified. For composite Ag-Cu-Ag NRs with s equal to 2.0 nm or smaller and k equal to 8 or smaller, a fcc-to-bct phase transition takes place that also involves the Cu domain. Within the same s range, the Cu domain is no longer affected by the fcc-to-bct transition when k becomes larger than 8. The Ag-Cu-Ag NRs with side length s larger than 2.0 nm and number k of Cu atomic planes around 10 also exhibits the same behavior. This is quite surprising, since the corresponding Ag NRs do not undergo any structural transformation. Therefore, it must be inferred that the phase transition is due to the central Cu domain. For all of the remaining Ag-Cu-Ag NRs, no phase transition occurs.

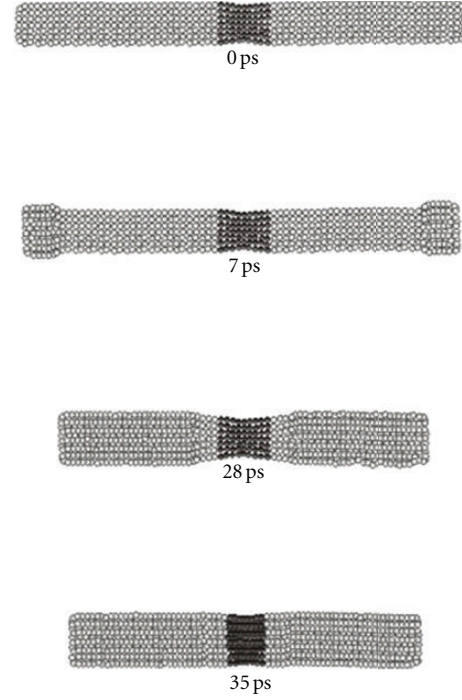


FIGURE 5: The atomic configurations of the composite Ag-Cu-Ag NR with sides about 1.2 nm long and 8 Cu atomic planes in the central region. Ag and Cu atoms are shown in light and dark gray, respectively. Configurations are taken at the times indicated.

For simplicity, hereafter the cases in which transformations take place will be indicated as A, B, and C. Case A will include the Ag-Cu-Ag NRs in which both Ag and Cu domains undergo a fcc-to-bct phase transition. Case B will refer to NRs in which only the Ag domain participates in the transition. Finally, Case C will refer to the NRs in which the Ag domains transform even though the corresponding Ag NRs do not.

4.1. Case A. The atomic configurations of the composite Ag-Cu-Ag NR with side length s equal to 1.2 nm and k equal to 8 are shown in Figure 5 at different times after the isolation from the parent matrix. It can be seen that, as in the case of Ag NRs, the fcc-to-bct phase transition starts at the Ag-free surfaces perpendicular to the main NR axis. Once the phase transition has started, the transition front propagates along the NR axis at rates of about 400 nm ns^{-1} . The Cu atomic planes in the central region do not arrest the transition front. On the contrary, it overcomes the strained coherent interfaces between Ag and Cu and forces the Cu domain to take a bct arrangement. The analysis of the arrangement of nearest neighbors indicates that the Cu bct phase exhibits elementary cell parameters a_{bct} and c_{bct} equal to about 0.309 and 0.261 nm, respectively. Correspondingly, the contraction of the Cu lattice along the main NR axis and its dilatation perpendicular to it, are similar in percentage to the ones observed in Ag NRs.

As a whole, case A NRs and Ag NRs share a similar behavior. The fcc arrangement is replaced by the bct one along the whole NR length, and the Ag-Cu interfaces keep

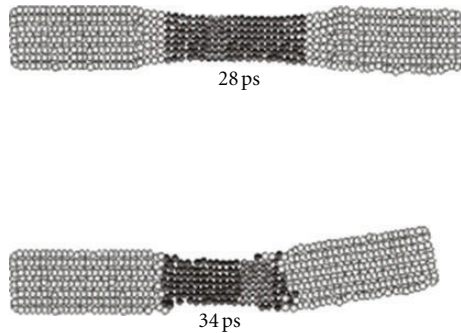


FIGURE 6: The atomic configurations of the composite Ag–Cu–Ag NR with sides about 1.2 nm long and 20 Cu atomic planes in the central region. Ag and Cu atoms are shown in light and dark gray, respectively. Configurations are taken at the times indicated.

coherent. After the transition, the composite Ag–Cu–Ag NRs still exhibit a thinner central region. Indeed, although it withstands considerable strain, the Cu domain exhibits elementary bct cell parameters smaller than Ag.

The difference between the elementary bct cell parameters of Ag and Cu depends on the size of the Cu domain. It decreases as the number k of Cu atomic planes decreases and almost disappears when k is equal to 2. The afore mentioned findings suggest that the behavior of case A NRs is dominated by the coherency of the Ag–Cu interfaces. In contrast, when the number k of Cu atomic planes increases, the Case A behavior is replaced by the Case B one.

4.2. Case B. As the number k of Cu atomic planes in the central region of the composite Ag–Cu–Ag NR with side length s equal to 2.0 nm becomes larger than 8, the fcc-to-bct phase transition no longer involves the Cu domain. The structural evolution of these NRs is exemplified by the atomic configurations shown in Figure 6, regarding the composite Ag–Cu–Ag NR with side length s equal to 1.2 nm and k equal to 20. The Ag–Cu–Ag NRs with s values equal to 1.6 and 1.2 nm and k values, respectively, equal to 8 and 10 exhibit a similar behavior.

In Case A and Ag NRs, the fcc-to-bct phase transition nucleates at the free Ag surfaces perpendicular to the main NR axis. As far as the transition fronts undergo their axial displacements within the Ag portions, the propagation rate is comparable with the one of about 400 nm ns^{-1} observed in Case A and Ag NRs. The fcc-to-bct phase transition progressively involves the entire Ag domains, but it arrests at the Ag–Cu interfaces. The Cu domain keeps its initial fcc structure, although disordering processes take place at interfaces. These determine the loss of interface coherency, and a modification of the overall structure of the NRs. The final configuration in Figure 6 clearly shows that the two Ag portions no longer share the same main axis, exhibiting a misalignment of about 10° .

A similar behavior is observed in all of the Case B NRs. The extent to which the NR structure is modified depends on the number k of Cu atomic planes. The smaller the Cu domain, the more disordered the final arrangement of the Cu and Ag portions.

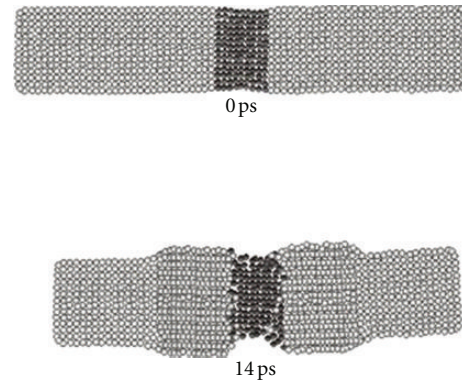


FIGURE 7: The atomic configurations of the composite Ag–Cu–Ag NR with sides about 2.4 nm long and 10 Cu atomic planes in the central region. Ag and Cu atoms are shown in light and dark gray, respectively. Configurations are taken at the times indicated.

The Ag–Cu interfaces rapidly disorder as the fcc-to-bct phase transition takes place. The structural modifications affecting the Ag domains induce a considerable strain on the adjacent Cu atomic planes. Although the Cu lattice is no longer able to follow the dilatation of the Ag one, the interfacial interactions are intense enough to induce the nucleation of lattice defects and the displacement of atomic species. This results in a limited mixing of Ag and Cu atoms at interfaces, aimed at lowering the surface energy.

4.3. Case C. A few composite Ag–Cu–Ag NRs with side length s larger than 2.0 nm also undergo structural modifications. In the light of the Ag NR behavior, this is somewhat unexpected. In fact, only Ag NRs with s values equal to 2.0 nm or smaller undergo a phase transition. Therefore, the phase transitions in the composite Ag–Cu–Ag NRs can be reasonably ascribed to the presence of the central Cu domain.

The observed structural modification is exemplified by the atomic configurations shown in Figure 7 for the composite Ag–Cu–Ag NR with side length s equal to 2.4 nm and 10 Cu atomic planes in the middle. The Ag end portions undergo the fcc-to-bct phase transition, whereas the Cu central domain is not involved. However, different from Case A and Case B NRs, the bct phase no longer nucleates at the free Ag surfaces perpendicular to the main NR axis. Rather, the phase transition starts in the neighborhood of the Ag–Cu interfaces. Thus, it appears that the transition behavior should be connected with the stress induced by the strained coherent Ag–Cu interface.

5. Composite Cu–Ag–Cu NRs

The composite Cu–Ag–Cu NRs have roughly the same size of the Ag–Cu–Ag ones, but opposite compositional profile. Simulations indicate that the central Ag domain still undergoes the fcc-to-bct phase transition, provided that the side length s is equal to 2.0 nm or smaller and the number k of Ag atomic planes is larger than 6. In the other cases, the Ag domain keeps its usual fcc structure.

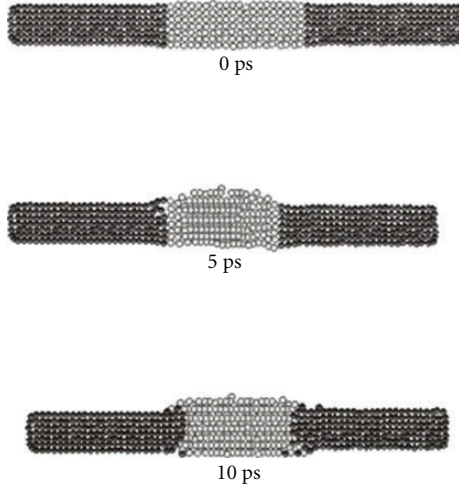


FIGURE 8: The atomic configurations of the composite Cu–Ag–Cu NR with sides about 1.2 nm long and 20 Ag atomic planes in the central region. Ag and Cu atoms are shown in light and dark gray, respectively. Configurations are taken at the times indicated.

The structural evolution of the Cu–Ag–Cu NR with side length s equal to 1.2 nm and number k of Ag atomic planes equal to 20 is exemplified by the atomic configurations shown in Figure 8. It can be seen that the phase transition nucleates homogeneously in the Ag domain. No transition front is observed. The coherency of Ag–Cu interfaces is rapidly lost, which induces the disordering of interfacial regions and the misalignment of Ag and Cu domains.

6. Discussion

The different behaviors exhibited by Ag and Cu NRs, as well as by composite Ag–Cu–Ag and Cu–Ag–Cu NRs, are determined by size effects. In the case of Ag and Cu NRs, size effects can be substantially identified with the stress f intrinsically associated with the NR free surfaces. The surface stress f can take quite large values, inducing a significant compressive stress σ_{NR} along the main NR axis. In turn, this compressive stress can be large enough to stabilize the bct structure over the fcc one. Provided that the cross-sectional area of the NRs becomes smaller than a threshold of about 4.0 nm^2 , a fcc-to-bct phase transition is actually observed in the case of Ag NRs. Conversely, no such transition takes place in the case of Cu NRs. In fact, Cu keeps its usual fcc structure irrespective of the NR cross-sectional area.

Although a similar mechanism can be expected to operate in composite Ag–Cu–Ag and Cu–Ag–Cu NRs, the situation is further complicated by the structural heterogeneity. In particular, it must be expected that size effects connected with the side length s of the NRs are modulated by the size, that is, the number k of atomic planes, of the central Cu or Ag domains. The numerical findings clearly show that, depending on the s and k values, the NRs can undergo a fcc-to-bct phase transition. This phase transition can involve either the whole NR or only the Ag domains. It must be noted that, different from the case of Ag NRs, Ag domains

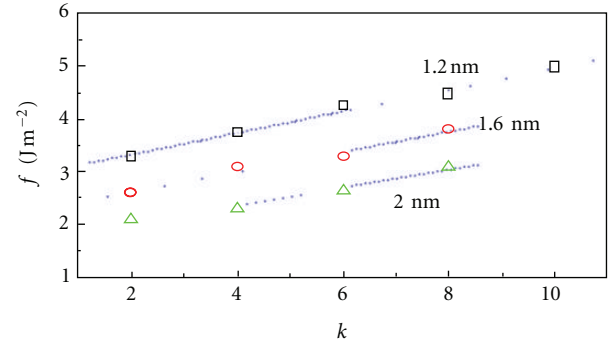


FIGURE 9: The average surface stress f as a function of the number k of Cu atomic planes for the Case A composite Ag–Cu–Ag NRs. Data refer to the case of NRs with side length s equal to 1.2, 1.6, and 2.0 nm as indicated. Best-fitted lines are also shown.

can undergo the fcc-to-bct phase transition also when their side length s is larger than 2.0 nm.

The average surface stress f for Case A composite Ag–Cu–Ag NRs that undergo the fcc-to-bct phase transformation is shown in Figure 9 as a function of the number k of Cu atomic planes. The f estimates exhibit a simple dependence on the size of the Cu domain, increasing almost linearly with k . The minimum f value allowing the fcc-to-bct phase transition amounts roughly to 2.1 J m^{-2} . This value is not far from the one observed in the case of Ag NRs, equal to about 1.7 J m^{-2} , and close to the f estimate obtained for Ag NRs submitted to a hydrostatic pressure of roughly 0.3 GPa [8]. The NRs with the shortest side length s exhibit an intrinsic surface stress f as large as 4.9 J m^{-2} . As a whole, it follows that the free surfaces of composite Ag–Cu–Ag are considerably more strained than the ones of the Ag NRs of similar size.

The large intrinsic surface stress f exhibited by case A NRs can be tentatively rationalized in terms of local strains generated by coherent Ag–Cu interfaces. The Cu fcc lattice has an elementary cell parameter of about 0.362 nm, remarkably smaller than the one of about 0.410 nm characteristic of the Ag fcc lattice. The difference between these two values induces tensile and compressive loadings, respectively, on the Cu and Ag domains, particularly in the region neighboring the coherent interface. Locally, such local strain further enhances the compressive stresses σ_{NW} , already present due to the reduced size of NRs.

A consequence of the large average values of the intrinsic surface stress f is the involvement of the central Cu domains of composite Ag–Cu–Ag NRs in the fcc-to-bct phase transition. This never occurs in bulk Cu phases and in Cu NRs, irrespective of their size. It follows that the relative stability of the bct Cu domain must be ascribed to a combination of effects connected with surface stresses and Ag–Cu coherent interfaces.

Case B and Case C NRs present different aspects. Cu domains keep their fcc structure unchanged despite the fcc-to-bct phase transition involving the Ag ones. This determines the release of the elastic energy associated with coherent Ag–Cu interfaces. Such energy was roughly estimated by calculating the potential energy difference between

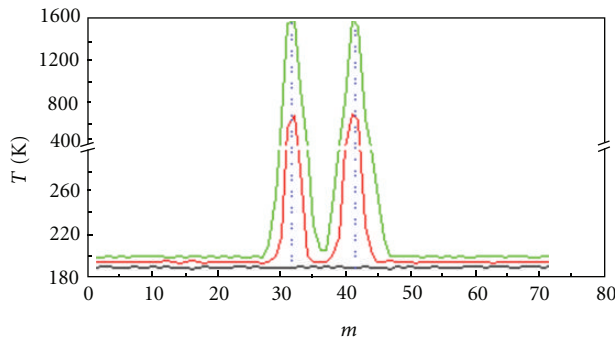


FIGURE 10: The average temperature T of the m individual atomic planes of the composite Ag–Cu–Ag NR with side length s equal to 1.6 and 10 Cu atomic planes. The vertical dotted lines ideally locate the Ag–Cu interfaces. The curves are downshifted of 5 and 10 K for avoiding superposition. From bottom to top, the data refer to the temperature profiles at the beginning of the fcc-to-bct phase transition in Ag end portions, after about 29 ps, and after about 30 ps. At longer times, the temperature of interfacial planes starts decreasing.

coherent and incoherent Ag–Cu interfaces. In turn, these were evaluated by comparing the total energies of Ag and Cu NRs of suitable size with the ones of composite Ag–Cu–Ag NRs of the same size containing either coherent or incoherent interfaces. The obtained energies for coherent and incoherent Ag–Cu interfaces with (100) topology amount roughly to 1.2 and 0.8 J m^{-2} respectively, in substantial agreement with literature values [26, 28]. It follows that the elastic energy released when the Ag domains of case B and case C NRs undergo the fcc-to-bct phase transition is on the order of 0.4 J m^{-2} . The same is true for the case of central Ag domains undergoing the fcc-to-bct transition in composite Cu–Ag–Cu NRs.

The elastic energy is released almost instantaneously at the phase transition. As a consequence, the local temperature T at Ag–Cu interfaces also rises almost instantaneously. Local temperatures T were estimated by monitoring the average kinetic energy in the m individual atomic planes forming the NRs [26]. The T estimates obtained at different times for the composite Ag–Cu–Ag NR with side length s equal to 1.6 nm and number k of Cu atomic planes equal to 10 are shown in Figure 10. It can be seen that the Ag and Cu planes at interfaces undergo a rapid T increase immediately after the loss of coherency at the Ag–Cu interfaces. The temperature T of the interfacial atomic planes rises up to about 1600 K, which is roughly 400 K points $T_{m,\text{Ag}}$ and $T_{m,\text{Cu}}$ of Ag and Cu, respectively. Although T keeps higher than $T_{m,\text{Ag}}$ and $T_{m,\text{Cu}}$ for about 5 ps only, such time interval is sufficient to allow a certain mobility to interface atoms, which undergo intermixing and disordering phenomena. The same phenomena occur in the other composite Ag–Cu–Ag NRs as well as in composite Cu–Ag–Cu NRs in which the central Ag domain undergoes the fcc-to-bct transition.

7. Conclusions

Numerical findings indicate that as the intrinsic surface stresses reach a threshold value, the fcc structure of Ag NRs

becomes unstable, and a fcc-to-bct phase transition takes place. The transition starts at the surfaces perpendicular to the main NR axis and propagates to the rest of the NR. Conversely, Cu NRs always keep the fcc structure.

Whereas the structural behavior of Ag and Cu NRs depends only on their size, in the case of composite Ag–Cu–Ag and Cu–Ag–Cu NRs, the size of the central Cu or Ag domains also plays an important role. Three different structural behaviors emerge in composite NRs as a function of the NR side length s and of the number k of atomic planes in the central Ag or Cu domain. The Ag–Cu–Ag NRs with side length $s \geq 2.4 \text{ nm}$ do not undergo structural modifications, in agreement with the case of Ag NRs of similar size. In contrast, an fcc-to-bct phase transition takes place in composite Ag–Cu–Ag NRs with side length $s \leq 2.0 \text{ nm}$ and 8 or 10 Cu atomic planes. In these cases, the transition also involves the central Cu domain, although the bct structure is unstable in both bulk Cu and pure Cu NRs of similar size.

The fcc-to-bct phase transition is also observed in Ag–Cu–Ag NRs with more than 10 Cu atomic planes and in Cu–Ag–Cu NRs with more than 6 Ag atomic planes. However, the transition only involves the Ag domains, leaving the Cu ones unaffected. The Ag–Cu interfaces lose their coherency and almost instantaneously release the associated elastic energy. The temperature of interfaces suddenly rises up to about 1600 K, which allows a significant local disordering and the loss of coaxiality of Ag and Cu domains.

Acknowledgments

A. Ermini, ExtraInformatica s.r.l., is gratefully acknowledged for his kind assistance and support. Financial support has been given by the University of Cagliari.

References

- [1] F. Baletto and R. Ferrando, “Structural properties of nanoclusters: energetic, thermodynamic, and kinetic effects,” *Reviews of Modern Physics*, vol. 77, no. 1, pp. 371–423, 2005.
- [2] R. Ferrando, J. Jellinek, and R. L. Johnston, “Nanoalloys: From theory to applications of alloy clusters and nanoparticles,” *Chemical Reviews*, vol. 108, no. 3, pp. 845–910, 2008.
- [3] P. Moriarty, “Nanostructured materials,” *Reports on Progress in Physics*, vol. 64, no. 3, pp. 297–381, 2001.
- [4] J. Jortner and C. N. R. Rao, “Nanostructured advanced materials. Perspectives and directions,” *Pure and Applied Chemistry*, vol. 74, no. 9, pp. 1491–1506, 2002.
- [5] G. A. Ozin and A. C. Arsenault, *Nanochemistry. A Chemical Approach to Nanomaterials*, RSC Publishing, Cambridge, UK, 2005.
- [6] Q. Guo, Y. Zhao, W. L. Mao, Z. Wang, Y. Xiong, and Y. Xia, “Cubic to tetragonal phase transformation in cold-compressed Pd nanocubes,” *Nano Letters*, vol. 8, no. 3, pp. 972–975, 2008.
- [7] K. Gall, J. Diao, M. L. Dunn, M. Hafel, N. Bernstein, and M. J. Mehl, “Tetragonal phase transformation in gold nanowires,” *Journal of Engineering Materials and Technology*, vol. 127, no. 4, pp. 417–422, 2005.
- [8] F. Delogu, “Numerical investigation of the cubic-to-tetragonal phase transition in Ag nanorods,” *Journal of Physical Chemistry*

- C, vol. 114, no. 8, pp. 3364–3370, 2010.
- [9] J. Lao and D. Moldovan, “Surface stress induced structural transformations and pseudoelastic effects in palladium nanowires,” *Applied Physics Letters*, vol. 93, no. 9, Article ID 093108, 2008.
 - [10] V. K. Sutrarakar and D. R. Mahapatra, “Comment on “surface stress induced structural transformations and pseudoelastic effects in palladium nanowires” [Appl. Phys. Lett. 93, 093108 (2008)],” *Applied Physics Letters*, vol. 97, no. 14, Article ID 146101, 2010.
 - [11] W. Tian, H. P. Sun, X. Q. Pan et al., “Hexagonal close-packed Ni nanostructures grown on the (001) surface of MgO,” *Applied Physics Letters*, vol. 86, no. 13, Article ID 131915, 3 pages, 2005.
 - [12] R. Ferrando, G. Rossi, F. Nita, G. Barcaro, and A. Fortunelli, “Interface-stabilized phases of metal-on-oxide nanodots,” *ACS Nano*, vol. 2, no. 9, pp. 1849–1856, 2008.
 - [13] G. J. Ackland and M. W. Finnis, “Semi-empirical calculation of solid surface tensions in body-centred cubic transition metals,” *Philosophical Magazine A*, vol. 54, no. 2, pp. 301–315, 1986.
 - [14] F. H. Streitz, R. C. Cammarata, and K. Sieradzki, “Surface-stress effects on elastic properties. I. Thin metal films,” *Physical Review B*, vol. 49, no. 15, pp. 10699–10706, 1994.
 - [15] J. Diao, K. Gall, and M. L. Dunn, “Atomistic simulation of the structure and elastic properties of gold nanowires,” *Journal of the Mechanics and Physics of Solids*, vol. 52, no. 9, pp. 1935–1962, 2004.
 - [16] V. Rosato, M. Guillope, and B. Legrand, “Thermodynamical and structural properties of f.c.c. transition metals using a simple tight-binding model,” *Philosophical Magazine A*, vol. 59, no. 2, pp. 321–336, 1989.
 - [17] F. Cleri and V. Rosato, “Tight-binding potentials for transition metals and alloys,” *Physical Review B*, vol. 48, no. 1, pp. 22–33, 1993.
 - [18] F. Delogu, E. Arca, G. Mulas, G. Manai, and I. Shvets, “Numerical investigation of the stability of Ag-Cu nanorods and nanowires,” *Physical Review B*, vol. 78, no. 2, Article ID 024103, 2008.
 - [19] F. Delogu, “Numerical simulation of the compression behavior of nanometer-sized Ag particles,” *Journal of Nanoscience and Nanotechnology*, vol. 9, no. 5, pp. 2944–2949, 2009.
 - [20] H. C. Andersen, “Molecular dynamics simulations at constant pressure and/or temperature,” *The Journal of Chemical Physics*, vol. 72, no. 4, pp. 2384–2393, 1980.
 - [21] S. Nosé, “A unified formulation of the constant temperature molecular dynamics methods,” *The Journal of Chemical Physics*, vol. 81, no. 1, pp. 511–519, 1984.
 - [22] M. Parrinello and A. Rahman, “Polymorphic transitions in single crystals: a new molecular dynamics method,” *Journal of Applied Physics*, vol. 52, no. 12, pp. 7182–7190, 1981.
 - [23] M. P. Allen and D. Tildesley, *Computer Simulations of Liquids*, Clarendon Press, Oxford, UK, 1987.
 - [24] J. Diao, K. Gall, and M. L. Dunn, “Surface-stress-induced phase transformation in metal nanowires,” *Nature Materials*, vol. 2, no. 10, pp. 656–660, 2003.
 - [25] G. E. Tommei, F. Baletto, R. Ferrando, R. Spadacini, and A. Danani, “Energetics of fcc and decahedral nanowires of Ag, Cu, Ni, and C 60: a quenched molecular dynamics study,” *Physical Review B*, vol. 69, no. 11, Article ID 115426, 2004.
 - [26] G. Mazzone, V. Rosato, M. Pintore, F. Delogu, P. Demontis, and G. B. Suffritti, “Molecular-dynamics calculations of thermodynamic properties of metastable alloys,” *Physical Review B*, vol. 55, no. 2, pp. 837–842, 1997.
 - [27] H. P. Klug and L. E. Alexander, *X-ray Diffraction Procedures*, John Wiley & Sons, New York, NY, USA, 1974.
 - [28] G. A. Adebayo and B. C. Anusionwu, “Dynamical properties of Ag-Cu binary alloy from molecular dynamics simulation,” *European Physical Journal B*, vol. 54, no. 4, pp. 423–427, 2006.